JOURNAL OF GUIDANCE, CONTROL, AND DYNAMICS
Vol. 24, No. 1, January–February 2001

Energy Approach to Flutter Suppression and Aeroelastic Control

Oddvar O. Bendiksen*
University of California, Los Angeles, California 90095-1597

Flutter is only possible in regions of the system phase space where the net aerodynamic work is positive over a suitably defined time interval, for example, one period of oscillation. In regions where the aerodynamic work is negative, no aeroelastic instabilities can occur, and the system is totally stable. In most cases, the unstable region is a finite subspace bounded by a closed flutter surface corresponding to neutral stability. The flutter subspace can be defined by a nonlinear aerodynamic work functional, whose magnitude represents the strength of the aeroelastic instability. A new flutter control concept based on aeroelastic energy principles is proposed, in which the main objective is to move the system out of the unstable region of phase space, by altering the critical aeroelastic mode. The classical picture of frequency coalescence flutter portrayed in aeroelasticity texts may be misleading and not a reliable guide in the unstable region. The more typical behavior appears to be one of frequency coalescence–divergence, where the mode frequencies tend to merge as the flutter boundary is approached from below, but then reverse direction and start to diverge after the system has crossed the flutter boundary and penetrated about 10–20% into the unstable region. This observation is of significance in the design of aeroelastic control laws for flutter suppression.

Nomenclature

a	=	speed of sound, location of elastic axis
C_L, C_M	=	lift and moment coefficients
c	=	airfoil or wing chord, $2b$
E, T, U	=	total, kinetic, and strain energy, respectively
h	=	plunge (bending) displacement at elastic axis (EA), positive down
K_h, K_α	=	typical section stiffness in bending and torsion, respectively
k	=	reduced frequency, $\omega b/U_\infty$
M	=	Mach number
m	=	mass per unit span
p	=	pressure
q	=	dynamic pressure, $\frac{1}{2}\rho_\infty U_\infty^2$
t	=	time
U_∞	=	freestream velocity at upstream infinity
$\bar{U}$	=	reduced velocity, $U_\infty/b\omega_\alpha$
W_A	=	aerodynamic work
α	=	angle of attack, torsion amplitude
θ	=	wing elastic twist
μ	=	mass ratio, $m/\pi\rho b^2$
ρ	=	air density
τ	=	nondimensional time, $\omega_\alpha t/2\pi$
ω	=	circular frequency, rad/s
ω_h, ω_α	=	uncoupled first bending and first torsion mode frequencies, respectively, in vacuum

Subscripts

F, D	=	conditions at flutter and divergence, respectively
∞	=	conditions at upstream infinity

Introduction

THE usefulness of energy concepts in explaining flutter is well-known, for example, see the classical texts of Fung[1] and Bisplinghoff and Ashley.[2] Previous studies of flutter from an energy standpoint include the works of Frazer and Duncan,[3] Garrick,[4] Barton,[5] Greidanus,[6] Crisp,[7] Carta,[8] and Nissim.[9] Because the elastic and inertial forces are conservative and do no work on the wing over a closed path in phase space, for example, over one cycle of a neutrally stable oscillation, the net work done by the aerodynamic forces on the wing must at least equal the work done by the internal dissipative (damping) forces, otherwise self-sustained oscillations would not be possible. Thus, the extraction of energy from the airstream is a necessary condition for flutter.

For the flutter instability to be dangerous, the supercritical region must allow the wing to extract energy at an increasing rate, to produce rapidly increasing flutter amplitudes. The more destructive types of flutter, such as bending–torsion flutter of slender wings, are of this type. Structural damping, or damping added via control forces, is relatively ineffective in suppressing bending–torsion flutter and may in some cases have a destabilizing rather than a stabilizing effect. This damping anomaly has been the subject of much discussion in the aeroelasticity literature over the years and is still relatively poorly understood from a physical standpoint. It is known to be intimately connected to the nonconservative nature of the unsteady aerodynamic forces, or stated differently, to the observation that the underlying boundary value problem is non-self-adjoint.

There are other flutter instabilities, usually weaker and thus not as destructive as bending–torsion flutter, where the effect of structural damping is both significant and predictable. Certain types of control surface and trim tab flutter fall into this category. Because often only a single degree of freedom is involved, the energy method provides a simple and effective tool for analyzing and explaining these types of flutter. The energy method can also provide valuable insight into nonlinear flutter problems in transonic flows, where limit cycles and flutter–divergence interactions can occur[10] and nonclassical flutter is possible through secondary Hopf bifurcations.[11]

This paper presents a new approach to the problem of flutter suppression and aeroelastic control, based on energy concepts and an aerodynamic work functional. Because flutter requires that the net aerodynamic work be positive over an oscillation period, one can show that for most wings such instabilities are possible only in a finite (compact) region of phase space, bounded by a closed flutter surface corresponding to neutral stability. This has often been overlooked in aeroelastic control studies. If the open-loop design is unstable, the energy approach provides a rational basis for aeroelastic control because it permits us to determine how the aeroelastic mode should be changed to stabilize the system. Furthermore, the aeroelastic energy functional allows us to determine the closest stable region of phase space, or the stable region that can be reached by expending the least amount of energy.

The use of simplified aerodynamic models is very prevalent in aeroservoelastic studies, and much research has been focused on reduced-order models for this purpose. In some cases, contradictory

Received 20 September 1999; revision received 27 March 2000; accepted for publication 28 March 2000.

*Professor, Department of Mechanical and Aerospace Engineering. Associate Fellow AIAA.

conclusions regarding the necessary or sufficient conditions for stabilization of even simple typical section models in incompressible flow have been reported. We believe that some of these discrepancies can be explained in terms of differences and/or inherent limitations of the individual aerodynamic models in the supercritical region. Unless the aerodynamic model provides consistent and reliable estimates of the absolute aerodynamic damping in the unstable region of the aeroelastic phase space, well beyond the linear flutter boundary, the aeroservoelastic predictions are likely to be of limited validity and thus also of limited practical value.

Aerodynamic Work Functional

Consider a thin slender wing, as shown in Fig. 1a. The aerodynamic work done over a specified time interval $[t_1, t_2]$ is given by

$$I = W_A = \int_{t_1}^{t_2} Q_i^A \dot{q}_i \, dt \tag{1}$$

where $Q_i^A(q_j, \dot{q}_j, \ddot{q}_j, \ldots)$ is the generalized aerodynamic force corresponding to the generalized aeroelastic coordinate q_i. Here and in what follows, the summation convention for repeated indices is implied, together with other common index notation conventions. The form of the aerodynamic force will be left unspecified for the moment, but it will be assumed that for a finite time interval $[t_1, t_2]$, the aerodynamic forces can be expanded in convergent Taylor series about the point $t = t_1$, or can be approximated in the form of asymptotic series or integrals involving only a finite number of time derivatives.

Equation (1) can be considered a functional, in the sense of the calculus of variations. It is natural to ask whether this functional possesses stationary points and if any of these represent maxima, minima, etc., of the corresponding aerodynamic work W_A. Because the unsteady aerodynamic forces are nonconservative, the aerodynamic work is not a conserved quantity, and hence, there is no energy conservation principle connected with this functional. However, this by itself does not preclude the possibility that the functional W_A as defined by Eq. (1) may possess stationary points. Obviously, if such stationary points exist, the corresponding extremals $q_i(t)$ of the aeroelastic system are of interest in the flutter control problem, because they are optimal aeroelastic path candidates in the sense that they minimize the energy transfer from the airstream to the structure during the specified time interval $[t_1, t_2]$.

To study this problem, we will consider the concept of a varied aeroelastic path, where each generalized aeroelastic coordinate q_i is given a small variation δq_i,

$$\tilde{q}_i(t) = q_i(t) + \varepsilon \eta_i(t) \equiv q_i(t) + \delta q_i(t) \tag{2}$$

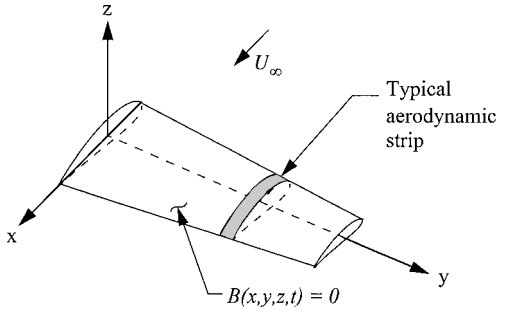

Fig. 1a Aircraft wing.

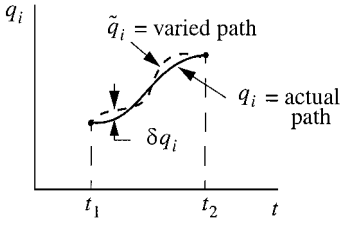

Fig. 1b Variation of aeroelastic path defined by the wing generalized coordinates $q_i(t)$.

as shown in Fig. 1b. Here $\varepsilon \ll 1$ and the $\eta_i(t)$, and hence also the δq_i, are smooth functions of t with continuous derivatives through second order, to satisfy the differentiability requirements of the equations of motion. By differentiating Eq. (2), we obtain the corresponding variations of the generalized velocities as $\delta \dot{q}_i = \varepsilon \dot{\eta}$, and so on for the higher derivatives.

A necessary condition for a minimum (or a maximum) of the aerodynamic work functional to exist is that the first variation of W_A must vanish,

$$\delta W_A = \int_{t_1}^{t_2} \left[Q_i^A \delta \dot{q}_i + \delta Q_i^A \dot{q}_i \right] dt = \int_{t_1}^{t_2} \left\{ Q_i^A \delta \dot{q}_i + \left(\frac{\partial Q_i^A}{\partial q_j} \delta q_j + \frac{\partial Q_i^A}{\partial \dot{q}_j} \delta \dot{q}_j + \frac{\partial Q_i^A}{\partial \ddot{q}_j} \delta \ddot{q}_j + \cdots \right) \dot{q}_i \right\} dt = 0 \tag{3}$$

Integrating by parts, one obtains for the various terms

$$\int_{t_1}^{t_2} Q_i^A \delta \dot{q}_i \, dt = Q_i^A \delta q_i \Big|_{t_1}^{t_2} - \int_{t_1}^{t_2} \frac{d}{dt}\left(Q_i^A\right) \delta q_i \, dt \tag{4}$$

$$\int_{t_1}^{t_2} \frac{\partial Q_i^A}{\partial \dot{q}_j} \dot{q}_i \delta \dot{q}_j \, dt = \frac{\partial Q_i^A}{\partial q_j} \dot{q}_i \delta q_j \Big|_{t_1}^{t_2} - \int_{t_1}^{t_2} \frac{d}{dt}\left(\frac{\partial Q_i^A}{\partial \dot{q}_j} \dot{q}_i \right) \delta q_j \, dt \tag{5}$$

$$\int_{t_1}^{t_2} \frac{\partial Q_i^A}{\partial \ddot{q}_j} \dot{q}_i \delta \ddot{q}_j \, dt = \frac{\partial Q_i^A}{\partial \ddot{q}_j} \dot{q}_i \delta \dot{q}_j \Big|_{t_1}^{t_2} - \frac{d}{dt}\left(\frac{\partial Q_i^A}{\partial \ddot{q}_j} \dot{q}_i \right) \delta q_j \Big|_{t_1}^{t_2} + \int_{t_1}^{t_2} \frac{d^2}{dt^2}\left(\frac{\partial Q_i^A}{\partial \ddot{q}_j} \dot{q}_i \right) \delta q_j \, dt \tag{6}$$

$$\cdots$$

and so on for higher derivatives. If we assume that the state of the system is known at $t = t_1$ and t_2 (as done in Hamilton's principle), then the boundary terms in Eqs. (4–6) vanish, and the following expression for the first variation of the aerodynamic work is obtained:

$$\delta W_A = \int_{t_1}^{t_2} \left\{ \left(\frac{\partial Q_i^A}{\partial q_j} \dot{q}_i - \frac{d}{dt}\left(\frac{\partial Q_i^A}{\partial \dot{q}_j} \dot{q}_i \right) + \frac{d^2}{dt^2}\left(\frac{\partial Q_i^A}{\partial \ddot{q}_j} \dot{q}_i \right) - \cdots \right) \delta q_j - \frac{d}{dt}\left(Q_i^A\right) \delta q_i \right\} dt \tag{7}$$

Because the variations δq_i are arbitrary, the fundamental lemma of the calculus of variations[12] requires that the following differential equations be satisfied so that $\delta W_A = 0$:

$$\frac{\partial Q_i^A}{\partial q_j} \dot{q}_i - \frac{d}{dt}\left(\frac{\partial Q_i^A}{\partial \dot{q}_j} \dot{q}_i + Q_j^A \right) + \frac{d^2}{dt^2}\left(\frac{\partial Q_i^A}{\partial \ddot{q}_j} \dot{q}_i \right) - \cdots = 0 \qquad j = 1, 2, \ldots, n \tag{8}$$

where n is the number of degrees of freedom. These are the Euler–Lagrange equations for the variational problem $\delta W_A = 0$, whose solutions define extremal paths for which the energy transfer from the fluid to the structure takes on stationary (and possibly minimum) values. Stated differently, the Euler–Lagrange equations give n necessary conditions that a candidate optimal path, in the energy sense, must satisfy to be a solution. Extensions to continuous systems ($n \to \infty$) is straightforward and will not be pursued here.

To determine whether a given solution yields a minimum of W_A, or a maximum, or neither, one must examine the second variation $\delta^2 W_A$, and it follows that

$$\delta^2 W_A > 0 \Rightarrow \min, \qquad \delta^2 W_A < 0 \Rightarrow \max \tag{9}$$

For simple aerodynamic theories, this test can be carried out analytically, but for realistic aeroelastic calculations using computational fluid dynamics (CFD) based aerodynamics, one must resort to numerical schemes to evaluate $\delta^2 W_A$. In principle, at least, this can always be done.

Aeroelastic Energy and Energy Criteria for Flutter

The total energy of the aeroelastic system (wing) can be written in Hamiltonian form as

$$E = \dot{q}_i p_i - L(q_j, \dot{q}_j, t) \tag{10}$$

where $L(q_j, \dot{q}_j, t) = T - V$ is the Lagrangian and $p_i = \partial L / \partial \dot{q}_i$ is the generalized momentum corresponding to the generalized coordinate q_i. Taking total derivatives with respect to time,

$$\frac{\mathrm{d}E}{\mathrm{d}t} = \frac{\partial E}{\partial t} + \frac{\partial E}{\partial q_i}\dot{q}_i + \frac{\partial E}{\partial p_i}\dot{p}_i = \frac{\mathrm{d}}{\mathrm{d}t}\left(\dot{q}_i \frac{\partial L}{\partial \dot{q}_i}\right) - \frac{\partial L}{\partial q_i}\dot{q}_i - \frac{\partial L}{\partial \dot{q}_i}\ddot{q}_i$$

$$= \dot{q}_i\left(\frac{\mathrm{d}}{\mathrm{d}t}\left(\frac{\partial L}{\partial \dot{q}_i}\right) - \frac{\partial L}{\partial q_i}\right) = \dot{q}_i Q_i^A = \frac{\mathrm{d}W_A}{\mathrm{d}t} \tag{11}$$

Here we have assumed that the only nonconservative forces present are the aerodynamic forces and that the Lagrangian does not explicitly depend on time. Equation (11) simply states that the work done by the aerodynamic forces goes into increasing the total energy of the wing, expressing the energy conservation law for the fluid–structure system.

Note that our viewpoint differs from that taken by Crisp,[7] who includes kinetic energies from the "apparent mass" terms and potential energies from "aerodynamic spring" terms in the definition of the total system energy. This in effect blurs the boundary between the structure and the fluid and makes it difficult to give a clear meaning to what exactly comprises the aeroelastic system. We believe that aeroelastic stability should be defined in terms of the total mechanical energy of the wing only, exclusive of aerodynamic terms. This definition agrees with the accepted engineering definition of flutter; namely, that flutter exists whenever the wing is able to extract energy from the airstream and thus increase its total energy $E = T + U$.

If one neglects the effect of structural damping, it follows that

$$E - W_A = T + U - W_A = E_0 = \text{const} \tag{12}$$

where E_0 is the initial energy of the wing at the zero reference point for the aerodynamic work functional, for example, at $t = t_1 = 0$. Consequently,

$$\frac{\mathrm{d}E}{\mathrm{d}t} = \frac{\mathrm{d}W_A}{\mathrm{d}t} = Q_i \dot{q}_i \equiv P_A \tag{13}$$

which is the rate at which the aerodynamic forces do net work on the wing, or the aerodynamic power P_A. It might seem that the correct physical and mathematical definition of flutter, or in this case the energy criterion for flutter, should be $\mathrm{d}E/\mathrm{d}t > 0$, but this is false. The fallacy here is the implicit assumption that E and W_A are monotonic functions of time, because time only enters implicitly through the dependence of the aerodynamic work on $q_j, \dot{q}_j, \ddot{q}_j, \ldots$. However, the generalized coordinates and velocities are oscillatory functions both in the subcritical as well as in the supercritical region. Hence, the time rate of change of E is typically both positive and negative over portions of a flutter oscillation (Fig. 2). Figure 2 shows the temporal behavior of E during transonic flutter of a three-dimensional wing.[13] From these observations, it should be clear that the correct definition of flutter in terms of the energy exchange between the fluid and the structure must involve an integrated aerodynamic power, in the form of the aerodynamic work functional defined in Eq. (1). The natural time interval $[t_1, t_2]$ in this context is the period $T = 2\pi/\omega$ of the critical aeroelastic mode.

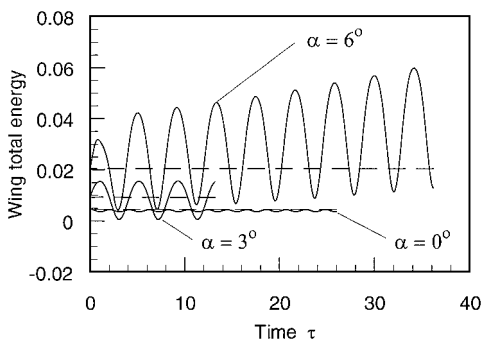

Fig. 2 Oscillatory behavior of $E = T + U$ during flutter; ONERA M6 wing at Mach 0.84 nonlinear three-dimensional Euler calculations for different angles of attack.[13]

In cases where the system matrices are time varying, either because of transient flight conditions or thermal effects or because of the presence of active or smart structures/actuators, the total energy is not conserved even in the absence of aerodynamic forces. Nevertheless, the total mechanical energy of the structural system is still the most meaningful gauge of stability in a practical engineering sense. The energy criterion proposed by Crisp[7] is somewhat different, but may lead to the same flutter boundary as the present criterion. The energy criterion proposed by Nissim[9] is an extension of the earlier linear aerodynamic work principle stated by Carta[8] for simple harmonic motion, but with aerodynamic control forces included. Although Nissim[9] is able to obtain a sufficient condition for stability in terms of the positiveness of the eigenvalues of a Hermitian matrix involving only the aerodynamic forces, it can be shown to be an overly restrictive condition, that is, it is not a necessary condition for stability.

Aerodynamic Work During Bending–Torsion Flutter

To focus on the essentials, we will examine a classical typical section model. The nondimensional equations of motion can be written in the form

$$\begin{pmatrix} 1 & x_\alpha \\ x_\alpha & r_\alpha^2 \end{pmatrix}\begin{Bmatrix} \ddot{h}(\tau)/b \\ \ddot{\alpha}(\tau) \end{Bmatrix} + \begin{pmatrix} \gamma_\omega^2 & 0 \\ 0 & r_\alpha^2 \end{pmatrix}\begin{Bmatrix} h(\tau)/b \\ \alpha(\tau) \end{Bmatrix} = \frac{\bar{U}^2}{\pi\mu}\begin{Bmatrix} -C_L(\tau) \\ 2C_M(\tau) \end{Bmatrix} \tag{14}$$

where the standard typical section notation has been used, with $\gamma_\omega = \omega_h/\omega_\alpha$, $\tau = \omega_\alpha t$, $\dot{\alpha} = \mathrm{d}\alpha/\mathrm{d}\tau$, etc., and the reduced velocity is defined by $\bar{U} = U_\infty/b\omega_\alpha$. If one specializes to the case of simple harmonic motion, as is done in classical linear flutter analyses, the lift and moment on the typical section model, per unit span, can be expressed in terms of the complex nondimensional coefficients A_{ij} of an aerodynamic matrix $\boldsymbol{A}$, as follows:

$$L = L_0 e^{i\omega t} = -\pi\rho_\infty b^3\omega^2[A_{11}(h/b) + A_{12}\alpha]$$

$$M = M_0 e^{i\omega t} = +\pi\rho_\infty b^4\omega^2[A_{21}(h/b) + A_{22}\alpha] \tag{15}$$

or in matrix form as

$$\begin{pmatrix} -Lb \\ M \end{pmatrix} = \pi\rho_\infty b^4\omega^2\begin{pmatrix} A_{11} & A_{12} \\ A_{21} & A_{22} \end{pmatrix}\begin{pmatrix} h/b \\ \alpha \end{pmatrix} = \pi\rho_\infty b^4\omega^2\boldsymbol{A}\boldsymbol{q}$$

$$\boldsymbol{q} = \begin{pmatrix} h/b \\ \alpha \end{pmatrix} \tag{16}$$

In the linear unsteady aerodynamic theories, the aerodynamic matrix coefficients in Eq. (15) depend only on the reduced frequency $k = \omega b/U_\infty$ and the Mach number $M_\infty = U_\infty/a_\infty$.

In the linear case, where the superposition principle remains valid (in the transonic region, this assumption is no longer valid), the total aerodynamic work can be considered a sum of two terms,

$$W_A^h = -\int_{t_1}^{t_2} Re\{L\}Re\{\dot{h}\}\,\mathrm{d}t, \qquad W_A^\alpha = \int_{t_1}^{t_2} Re\{M\}Re\{\dot{\alpha}\}\,\mathrm{d}t \tag{17}$$

representing the aerodynamic work done by the airstream on the wing section through the plunging and torsional motions, respectively. Here, real parts must be taken of the individual factors, if they are expressed in complex notation, because the differential work expressions are quadratic forms. If we assume simple harmonic motion,

$$h(t) = h_0 e^{i\omega t}, \qquad \alpha(t) = \alpha_0 e^{i(\omega t - \phi)} \tag{18}$$

where the bending and torsion amplitudes h_0 and α_0 are considered real and ϕ is the phase angle by which torsion lags bending, then the integrals in Eq. (17) can be evaluated in terms of the aerodynamic coefficients A_{ij} and the parameters of the system. When integrating over one period of oscillation, $t_1 = 2m\pi/\omega$, $t_2 = 2(m+1)\pi/\omega$, the work per unit span becomes

$$\Delta W_A^h = \pi^2 \rho_\infty b^4 \omega^2 \bar{h}_0 \left[A_{11}^I \bar{h}_0 - \left(A_{12}^R \sin\phi - A_{12}^I \cos\phi \right) \alpha_0 \right] \quad (19)$$

$$\Delta W_A^\alpha = \pi^2 \rho_\infty b^4 \omega^2 \alpha_0 \left[\left(A_{21}^R \sin\phi + A_{21}^I \cos\phi \right) \bar{h}_0 + A_{22}^I \alpha_0 \right] \quad (20)$$

where $\bar{h}_0 = h_0/b$ is the nondimensional bending amplitude and the R and I superscripts denote real and imaginary parts, respectively. Note that Eqs. (19) and (20) include coupling terms between bending and torsion, representing the work done on the bending mode due to the forces (lift) induced by torsion, and vice versa. The total aerodynamic work per cycle of oscillation is then

$$\Delta W_A = \Delta W_A^h + \Delta W_A^\alpha = \pi^2 \rho_\infty b^4 \omega^2 \alpha_0^2 F(\xi, \phi, k, M_\infty)$$

$$F(\xi, \phi, k, M_\infty) = A_{11}^I \xi^2 + \left\{ \left(A_{12}^I + A_{21}^I \right) \cos\phi - \left(A_{12}^R - A_{21}^R \right) \sin\phi \right\} \xi + A_{22}^I \quad (21)$$

where $\xi = h_0/(b\alpha_0)$ is the nondimensional amplitude ratio, bending to torsion. Equivalent expressions to Eq. (21) have also been derived by Greidanus[6] and Carta.[8]

We note from Eq. (21) that for a given amplitude of torsional motion, the aerodynamic work per unit span and cycle of oscillation is proportional to the nondimensional function $F(\xi, \phi, k, M_\infty)$, which in turn is a function of four variables, ξ, ϕ, k, and M_∞. Only the first three are related to the aeroelastic mode. For the linear case under consideration, the flutter boundary is given by the solution(s) to the equation

$$\overline{\Delta W_A} = \frac{\Delta W_A}{\pi^2 \rho_\infty b^4 \omega^2 \alpha_0^2} \equiv F(\xi, \phi, k, M_\infty) = 0 \quad (22)$$

where $\overline{\Delta W_A}$ is the nondimensional aerodynamic work per cycle and is identical to the function F. For the flutter solution(s) to have physical significance, that is, be realizable, the variables ξ, ϕ, and k must also satisfy the aeroelastic equations of motion. However, without actually solving the aeroelastic equations, one can examine the possible solutions of Eq. (22) and identify those regions of phase space where the solutions are real with $\xi \geq 0$ (flutter is possible) and those regions where no real solutions with $\xi \geq 0$ exist (flutter is impossible). The idea here is to partition the phase space of possible flutter solutions into a stable region, where no flutter can occur, and an unstable region, separated by the flutter boundary given by Eq. (22).

To show that the flutter surface given by Eq. (22) is a closed surface for fixed reduced frequency and Mach number, consider first the case where the phase ϕ is kept fixed in Eq. (22), then $F = 0$ results in a quadratic equation for the critical amplitude ratio

$$a\xi^2 - (b\sin\phi + c\cos\phi)\xi - d = 0 \quad (23)$$

$$a = A_{11}^I, \qquad b = A_{12}^R - A_{21}^R$$

$$c = -\left(A_{12}^I + A_{21}^I \right), \qquad d = -A_{22}^I \quad (24)$$

In incompressible flow, the coefficients can be expressed as

$$a = -(2/k)F(k), \qquad b = -(2/k^2)F(k) + (2/k)G(k)$$

$$c = 1/k + (2/k^2)G(k) + (1-2a)(1/k)F(k)$$

$$d = (1/k)\left(\tfrac{1}{2} - a\right) - (1/k^2)(1+2a)G(k) - (1/k)(1+2a)\left(\tfrac{1}{2} - a\right)F(k) \quad (25)$$

where F and G are the real and imaginary parts of the Theodorsen function

$$C(k) = \frac{H_1^{(2)}(k)}{H_1^{(2)}(k) + iH_0^{(2)}(k)} = F(k) + iG(k) \quad (26)$$

Here, $H_n^{(2)}(k) = J_n(k) - iY_n(k)$ is the Hankel function of the second kind, of order n, and $J_n(k)$ and $Y_n(k)$ are the corresponding Bessel functions of the first and second kind, respectively. The coefficients of Eq. (23) are real, and the two solutions

$$\xi_{1,2} = \left(b\sin\phi + c\cos\phi \pm \sqrt{(b\sin\phi + c\cos\phi)^2 + 4ad} \right) / 2a \quad (27)$$

are either both real or both complex, according to whether

$$(b\sin\phi + c\cos\phi)^2 + 4ad \geq 0 \qquad \text{or}$$

$$(b\sin\phi + c\cos\phi)^2 + 4ad < 0 \quad (28)$$

respectively. If the radicand vanishes, the two roots are identical.

Similarly, if the amplitude ratio ξ is fixed and the phase ϕ is varied to satisfy Eq. (22),

$$b\sin\phi + c\cos\phi = a\xi - d/\xi \quad (29)$$

For cases of practical interest, this equation typically has two real roots in the primary interval $0 \leq \phi < 360$ deg. For fixed k and M_∞, the loci of the roots of Eq. (22) defining the flutter boundary form a closed curve, as shown in Fig. 3a. Figure 3b shows the aerodynamic work function F and illustrates that the unstable region is a finite region of the phase space. Figure 4 shows the results of calculations

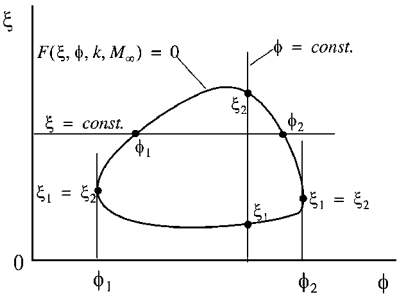

Fig. 3a Typical locus of $F = 0$, defining neutral stability for fixed k and M_∞ (flutter boundary) in two-dimensional phase space.

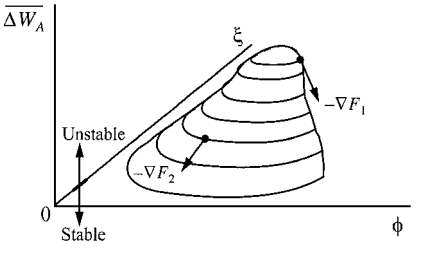

Fig. 3b Corresponding aerodynamic energy surface.

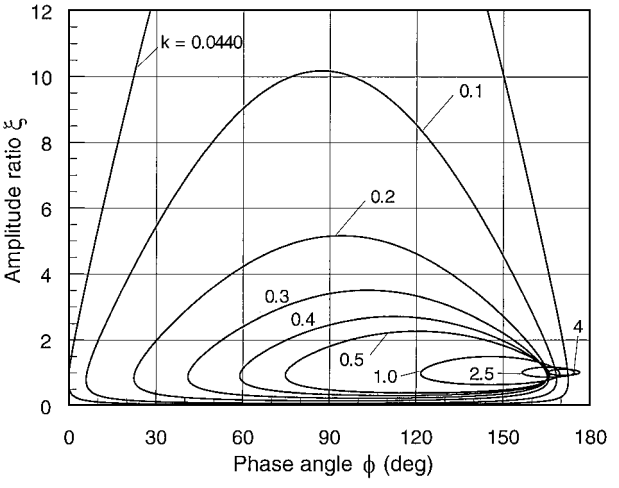

Fig. 4 Loci of roots of the aerodynamic work function F for bending–torsion oscillations in incompressible flow, calculated using Eqs. (25–27) with $a = -0.5$.

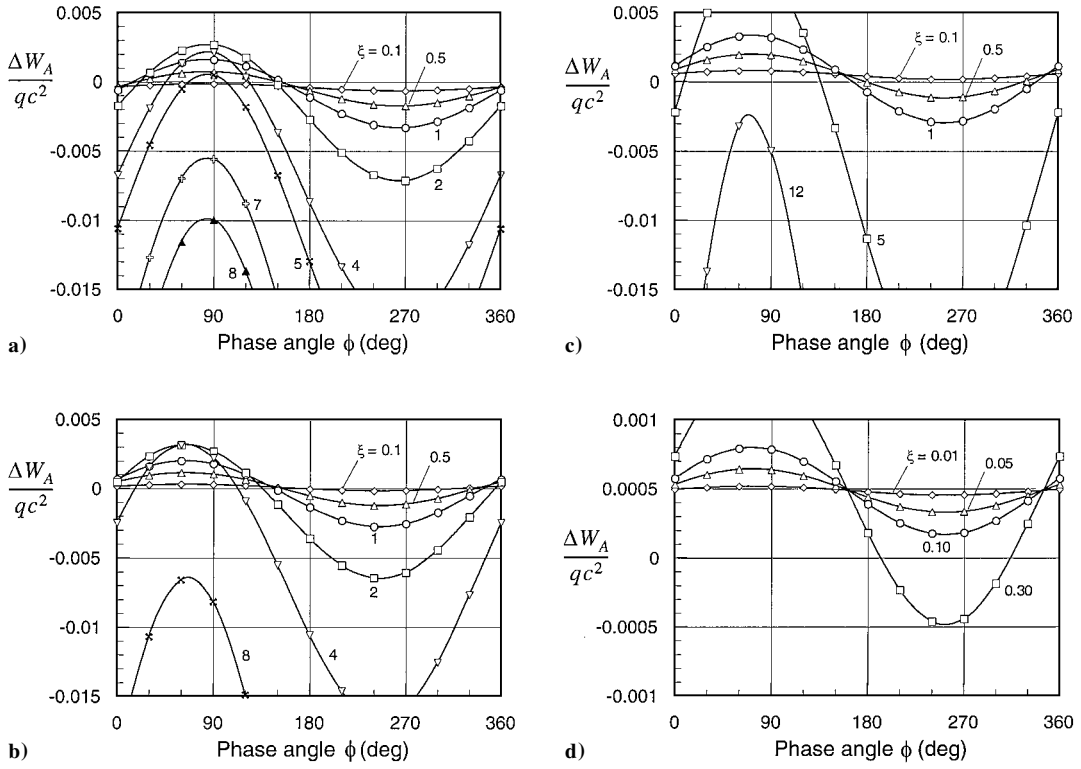

Fig. 5 Aerodynamic work per cycle, per unit span, calculated for an NACA 64A006 typical section with elastic axis at 0.4*c*: a) $M_\infty = 0.5, k = 0.2$; b) $M_\infty = 0.85, k = 0.2$; c) $M_\infty = 0.85, k = 0.1$; d) same as c) for low values of ξ.

for the incompressible case, based on the Theodorsen theory for a typical section [Eqs. (25–27)] using the double precision IMSL library to evaluate the Bessel functions. For a given reduced frequency, the section is unstable for points (ξ, ϕ) that fall inside the corresponding closed curve in Fig. 4. Note that for almost the entire range of reduced frequencies, that is, $0.044 < k < \infty$, the unstable phase angles fall in the interval $0 < \phi < 180$ deg; thus, flutter at $M_\infty = 0$ is only possible if torsion lags bending. This also appears to be the case for most subsonic Mach numbers, but is no longer true in the transonic regime.

In the quasistatic aerodynamic approximation, the lift and moment coefficients are given by

$$C_L = C_{L\alpha}[\alpha + \dot{h}\omega_\alpha / U_\infty], \qquad C_M = (\bar{e}/2)C_{L\alpha}[\alpha + \dot{h}\omega_\alpha / U_\infty] \tag{30}$$

where $\bar{e}$ is the offset between the aerodynamic center and the elastic axis, nondimensionalized with respect to the semichord b. If one sets $h = h_0 e^{p\tau}$ and $\alpha = \alpha_0 e^{p\tau}$, the characteristic equation becomes

$$Ap^4 + Bp^3 + Cp^2 + Dp + E = 0 \tag{31}$$

$$A = r_\alpha^2 - x_\alpha^2, \qquad D = \left(r_\alpha^2 \middle| \bar{U}\right)\lambda$$

$$B = \left(r_\alpha^2 + \bar{e}x_\alpha\right)\lambda/\bar{U}, \qquad E = \gamma_\omega^2\left(r_\alpha^2 - \bar{e}\lambda\right)$$

$$C = \left(1 + \gamma_\omega^2\right)r_\alpha^2 - (\bar{e} + x_\alpha)\lambda, \qquad \lambda = (\bar{U}^2/\pi\mu)C_{L\alpha} \tag{32}$$

where λ is a flutter or bifurcation parameter. The characteristic equation (31) has four roots, which occur as two complex conjugate pairs,

$$p_{1,2} = p_{1_R} \pm i\omega_1, \qquad p_{3,4} = p_{2_R} \pm i\omega_2 \tag{33}$$

because the coefficients of Eq. (31) are real. The two complex pairs correspond to the two aeroelastic modes in the system, that is, the bending and torsion branches.

Although the quasistatic approximation has been used in some aeroservoelastic studies to study the effectiveness or suitability of various control laws, our calculations indicate that it is unsuitable for this purpose. The main reason appears to be that the aerodynamic damping associated with the two aeroelastic branches, one stable and one unstable, may be poorly modeled by the quasi-static approximation. This is especially true if the aerodynamic damping terms are neglected, in which case the model gives unrealistic root loci in the supercritical region.

In the transonic region, the aerodynamic work must be obtained through direct numerical integration of Eq. (1), using CFD methods to obtain the unsteady aerodynamic forces. Examples of such nonlinear Euler calculations for an NACA 64A006 typical section are shown in Fig. 5. Nonlinear effects due to shock motion are sufficiently strong to cause a noticeable first-order violation in the superposition principle [implied in Eqs. (17) and (21)], and the unstable region is enlarged. In all cases, the unsteady Euler equations were time marched to get W_A, while keeping the torsional amplitude fixed at 1 deg about a mean angle of attack of $\alpha_0 = 3$ deg. Note the strong almost sinusoidal dependence of ΔW_A on the phase angle ϕ and the characteristic peak instability at positive angles in the 60–90 deg range. These calculations verify the hypothesis that the typical section can be stabilized at any ϕ by increasing the bending–torsion amplitude ratio ξ sufficiently so that the mode (ξ, ϕ) falls outside the closed flutter curve illustrated in Fig. 2a. This can most easily be done by suppressing the torsion component of the flutter mode.

Classical Flutter Revisited

Coalescence or Coalescence–Divergence Flutter?

Classical bending–torsion flutter is often described as a coalescence flutter, because in the absence of damping the frequencies of the bending and torsion modes merge at the flutter point. For incompressible or low subsonic flows, the typical section model with quasi-static aerodynamics provides a reasonable mathematical model for explaining how this instability comes about and its overall qualitative characteristics. A representative example of such a calculation is shown in Fig. 6, which is taken from Bisplinghoff and Ashley.[2] The same example is also used to describe the basic physics behind bending–torsion flutter in the text by Dowell et al.[14] Here, we have recalculated the stability behavior of this model, by solving the characteristic equation (31) numerically, using the double precision IMSL routine DZANLY. With the aerodynamic damping terms included, flutter occurs at $\bar{U} = 0.87$, which is in agreement with

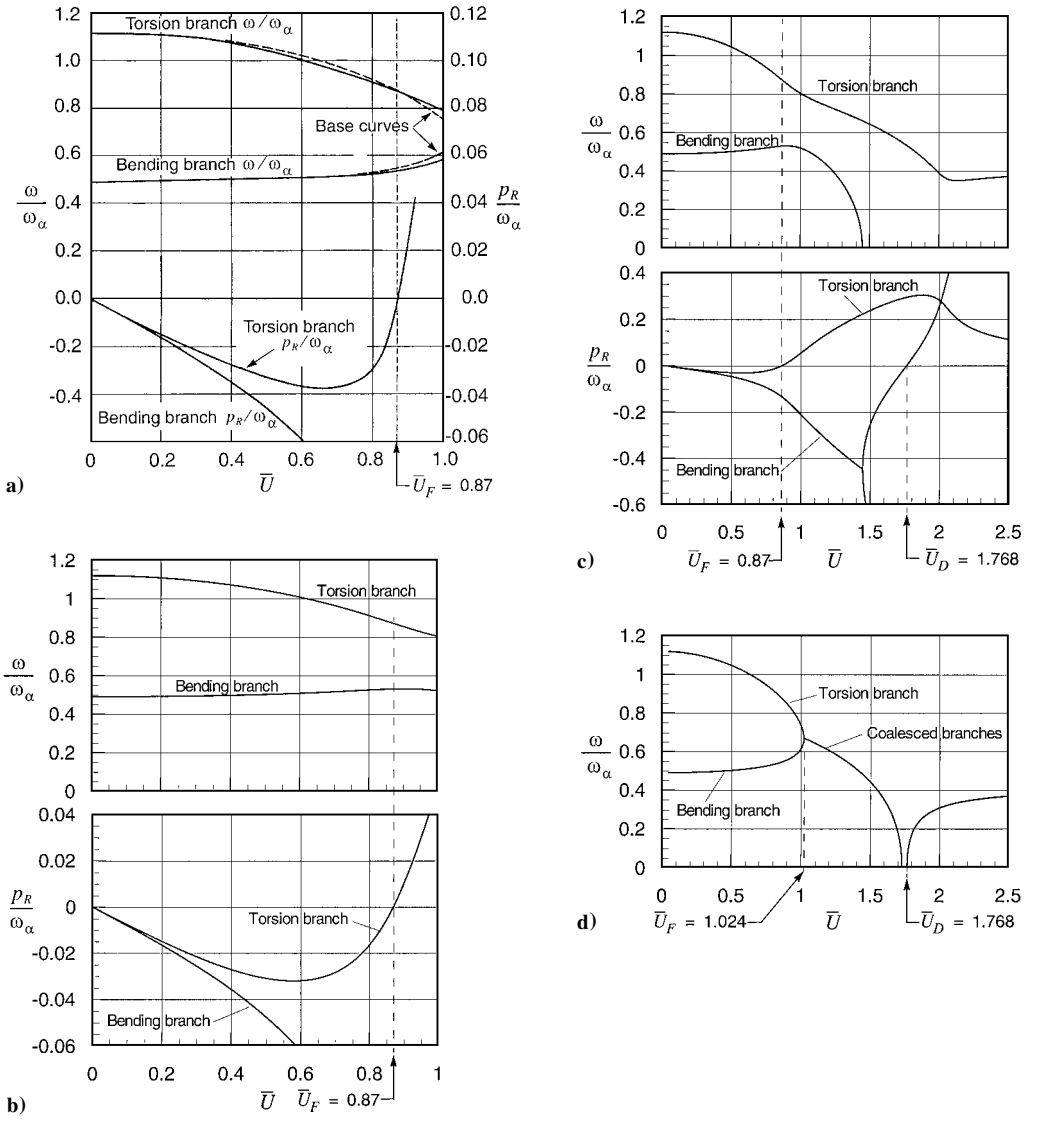

Fig. 6 Reexamination of the classical bending–torsion flutter example in Fig. 6-30 of Bisplinghoff and Ashley[2]: a) frequency and damping of aeroelastic modes vs reduced airspeed, from Ref. 2; b) present calculations, solving characteristic equation (31) numerically using IMSL routine DZANLY; c) present calculations extended into the supercritical region; d) present calculations, extended into supercritical region with the aerodynamic damping terms neglected; $\bar{e} = 0.4$, $r_\alpha = 0.5$, $x_\alpha = 0.2$, $\omega_h/\omega_\alpha = 0.5$, $\theta = 10$, and $C_{L_\alpha} = 2\pi$.

Fig. 6-30 of Ref. 2. Without aerodynamic damping, the present calculations yield a flutter speed of $\bar{U} = 1.024$. No value for this case is given in Ref. 2, but Ref. 14 gives 1.06 for the undamped flutter speed. Note that the value given for x_α in Refs. 2 and 14 appears in error, with Ref. 2 listing a value of 0.5, whereas Ref. 14 lists 0.05. However, neither of these values gives the stated flutter speed of 0.87. After some trial and error calculations, it was concluded that the correct value should (in all probability) be $x_\alpha = 0.20$, which is the value used in the present calculations.

Figure 6b shows our present recalculation for the subcritical region, with the aerodynamic damping terms included. Small differences are noted in the frequency behavior of the bending mode immediately past the flutter boundary. There are also slight differences in the subcritical damping levels of the torsion branch, compared to Fig. 6-30 of Ref. 2, here reproduced as Fig. 6a. The supercritical behavior of this aeroelastic model is shown in Fig. 6c and is very different from what is suggested in Fig. 6a. It is often implicitly assumed, and sometimes explicitly stated, that the aeroelastic mode frequencies in the supercritical flutter region approach an asymptote from above and below, respectively. This is certainly not true in the present example, nor was it found to be true in a large number of other typical section models examined. Instead, the prevailing behavior can best be described as coalescence-divergence flutter, where the mode frequencies tend to merge as the flutter boundary is approached from below, but then reverse direction and start to diverge after the system has crossed the flutter boundary and penetrated roughly 10–20% into the unstable region.

One possible explanation for this surprising behavior is that the quasi-static approximation is unrealistic and that calculations using a better aerodynamic model would reveal a more familiar frequency coalescence behavior. This is at the moment an open question; however, for all wings where the divergence speed is not too far above the flutter speed, at least one of the aeroelastic mode frequencies must start to turn downward, toward zero, when the airspeed is not too far beyond the flutter speed. Because there appears to be no physical or mathematical reason why both mode frequencies should go to zero at the divergence speed, frequency divergence in the supercritical region must be expected somewhere between the flutter speed and the divergence speed.

The calculated supercritical aeroelastic eigensolution for this very simple model reveals another surprise. From Fig. 6c it can be seen that the frequency of the bending mode reaches zero at $\bar{U} = 1.45$, although an examination of the aeroelastic eigenvalues reveals that this is not a divergence point. Instead, at this airspeed the imaginary part of the complex conjugate pair of roots corresponding to the bending branch vanishes, leaving two identical negative (stable) real roots. As the airspeed is increased further, these two real roots split apart, with one becoming more negative while the other

root moves in the positive direction. At $\bar{U} = 1.768$ the latter root crosses zero and divergence occurs. This divergence speed agrees with the torsional divergence speed calculated from the classical formula, based on static equilibrium considerations. Surprisingly, we see from Fig. 6c that the aeroelastic eigenvalue responsible for the divergence instability belongs to the bending branch, not the torsion branch. Also note that although the condition $\omega \rightarrow 0$ is a necessary condition for divergence, it is not a sufficient condition. In addition, one must have $Re(p) > 0$.

Figure 6d shows the corresponding root loci if the aerodynamic damping terms are neglected in the quasi-static approximation. In this case the two mode frequencies merge at the flutter point and remain together in the supercritical region, where they gradually decrease to zero. At $\bar{U} = 1.732$, or about 5% below divergence, both frequencies have reached zero. Instead of two complex conjugate pairs of eigenvalues, we now have four real roots, which start out as two identical pairs $\pm p_R$. As the airspeed is increased further, the pairs diverge into four distinct real roots of the form $\pm p_{1_R}$ and $\pm p_{2_R}$, and at the classical divergence speed $\bar{U} = 1.768$, the roots $\pm p_{1_R}$ change into a purely imaginary complex conjugate pair of the form $\pm i\omega_1$.

For aeroservoelastic problems, where the postcritical flutter behavior is of importance in designing control laws, the message from this example should be one of caution. Simplified aerodynamic models that do a reasonable job of predicting the subcritical root loci and the flutter speed may nevertheless predict a totally wrong aeroelastic eigensolution in the supercritical region, especially at airspeeds significantly past the flutter boundary.

Single-Degree-of-Freedom Flutter

In incompressible or subsonic linearized flow, single-degree-of-freedom (SDOF) torsional flutter is possible only for rather unusual combinations of parameters. According to Fung,[1] these include a rotational axis forward of the one-quarter chord, but not too far ahead of the leading edge, and a very low reduced frequency. The energy method is an effective tool for analyzing the conditions under which SDOF flutter is possible, because the mode shape is known. The present calculations (Fig. 4) indicate that SDOF torsional flutter in incompressible flow is only possible for $k \leq 0.0440$, whereas Greidanus[6] obtained the critical range as $k < 0.0435$ (see Fung[1]). Note that for $k \leq 0.0440$, the instability loop intercepts the $\phi = 0$ axis, and a point located at x on the airfoil or its extension has the vertical downward displacement

$$-z = h + (x - ba)\alpha = [h_0 + (x - ba)\alpha_0]e^{i\omega t} \qquad (34)$$

which vanishes when $x = ba - h_0/\alpha_0 = b(a - \xi)$. The motion is then equivalent to a pure torsional motion about an axis at that point, and this motion is unstable for amplitude ratio(s) ξ that fall inside the flutter loop at $\phi = 0$. This relation then gives the range of axis positions for which SDOF torsional flutter is possible in incompressible flow.

At transonic Mach numbers, however, SDOF torsional flutter becomes possible for typical section parameters and reduced frequencies of practical interest, as is evident from Figs. 5b–5d. Usually, this instability only occurs at nonzero angles of attack and is, thus, a nonlinear effect. Results from SDOF nonlinear Euler calculations for the NACA 64A006 airfoil oscillating around an axis at $0.4c$ are shown in Fig. 7. At Mach 0.85, the aerodynamic work per cycle is clearly positive for mean (trim) angles of attack above about 2 deg and reduced frequencies below about 0.15. It is believed that this SDOF instability interacts with the weak divergence also present at Mach 0.85, to produce the (apparently) chaotic motion reported by Kousen and Bendiksen[10] and Bendiksen.[11] Additional calculations (not shown) indicate that the SDOF torsional instability extends to Mach numbers well below the transonic region, at least to Mach 0.50 for trim angles of attack of 5 deg.

From a practical standpoint, the existence of such a SDOF torsional instability may seem unimportant because its strength is likely to be much weaker than the corresponding bending–torsion instability. However, caution is in order because this additional unstable root will most likely interact with the bending–torsion instability

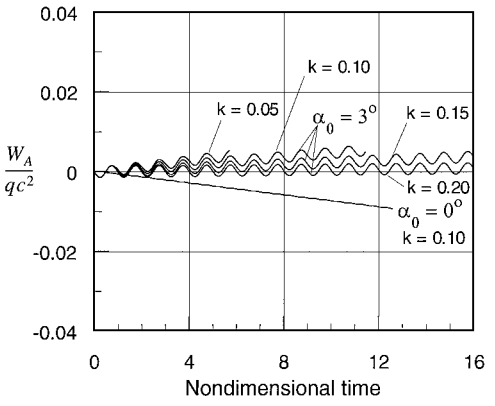

Fig. 7 Aerodynamic work vs time for SDOF torsional oscillations of the NACA 64006 typical section model at Mach 0.85.

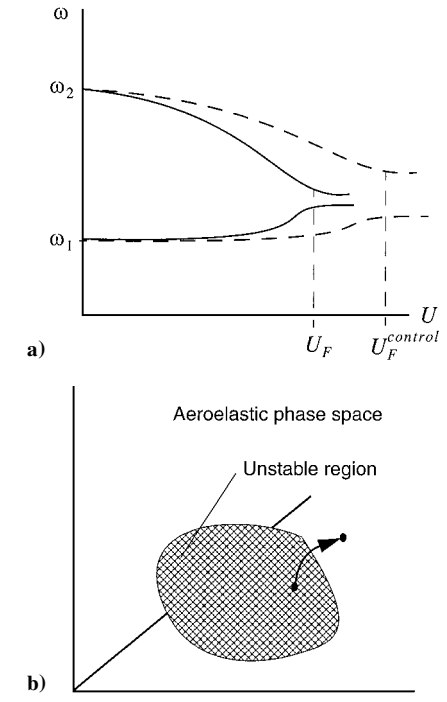

Fig. 8 Two physical approaches to flutter control: a) impose control forces to separate (or prevent merging of) the aeroelastic frequencies and b) use aeroelastic mode control to change the critical aeroelastic mode and drive the mode out of the unstable region $\Delta W_A > 0$ and into a stable region $\Delta W_A < 0$ of the aeroelastic phase space.

and, thus, affect the bending–torsion flutter speed. Also, the torsion instability may contribute to the limit cycle oscillation (LCO) phenomena observed in certain fighter aircraft at high subsonic and transonic Mach numbers.

Flutter Control

Flutter control schemes can be classified into two groups: 1) control schemes that exploit the fundamental physics of the aeroelastic problem in selecting the control laws, for example, the tendency toward frequency coalescence in binary bending–torsion flutter, and 2) control schemes that treat the aeroelastic system as just another plant that can be identified and controlled by the methods of modern control theory.

We will only discuss schemes of the first class, to keep in line with the primary objective of this paper. Two control concepts or approaches, illustrated schematically in Fig. 8, will be considered.

Aeroelastic Frequency Control

The first approach is based on the observation that in the case of classical bending–torsion flutter, there is a strong tendency for the aeroelastic mode frequencies to merge or coalesce as flutter is

approached. The idea is then to try to prevent this frequency merging, by imposing suitable control forces, in the hope that this will prevent or at least delay the onset of flutter, as shown in Fig. 8a. This control concept is based on the assumption that the supercritical aeroelastic behavior of the wing is similar to its subcritical behavior, that is, that the aeroelastic mode frequencies continue to merge past the flutter boundary. However, if the frequency behavior in the supercritical region is of the divergence type, then this control strategy is likely to meet with difficulty.

Although the frequency separation idea is simple and easy to understand, it is not easy to implement in a workable control scheme, for example, see the discussion in Ref. 15. In that study, a number of control laws and performance metrics were considered in the flutter suppression of a strain-actuated wing. The test results showed (not surprisingly) that increasing the modal damping was ineffective in delaying flutter onset. Frequency separation was concluded to hold more promise, but was found to be "not an easily codifiable concept" from an implementation standpoint.

Aeroelastic Mode Control

The idea behind aeroelastic mode control, Fig. 8b, is to force the system into a stable region (subspace) of the phase space by altering the aeroelastic mode (bending–torsion amplitude ratio and phase), using the minimum control effort possible. For the most important case of binary bending–torsion flutter, topological maps of the aerodynamic work functional W_A can be constructed as surfaces of constant aerodynamic work per unit time, in a suitably defined phase space. This functional can be calculated using analytical methods or CFD or determined experimentally in a wind tunnel. An aeroelastic energy norm can then be defined for the system, which provides a rigorous basis for aeroelastic stability analyses and for formulating the aeroservoelastic problem as an extremum problem. If the open-loop design is unstable, W_A can be used to determine how the aeroelastic mode should be changed to stabilize the system. The strength of a potential instability in a given region of phase space can be calculated and the closest stable region of phase space identified. Using numerical optimization techniques, one can also determine the stable region that can be reached by expending the least amount of control energy.

This control approach is conceptually different from the frequency control scheme shown in Fig. 8a because it is based on altering the critical aeroelastic mode, rather than on trying to separate the frequencies of the interacting modes. Although the tendency for the mode frequencies to merge is a characteristic of bending–torsion flutter, it is a symptom rather than the primary cause of the instability. The mechanism behind bending–torsion flutter is the ability of the coupled fluid–structure system to alter the critical aeroelastic mode in such a manner that net energy is extracted from the airstream, over a period of oscillation. This aeroelastic energy flow is sensitive to the bending–torsion modal parameters, that is, amplitude ratio $h/b\alpha$ and phase ϕ, and also to Mach number and reduced frequency. By altering the amplitude ratio of the aeroelastic mode, and or the bending–torsion phase, the ability of the mode to extract energy from the airstream can be reduced significantly, thus stabilizing the mode.

Results from a large number of aeroservoelastic calculations on typical section models as well as three-dimensional wings suggest that bending–torsion flutter can be suppressed by using dynamic twist control to limit the torsion component of the flutter mode.[13,16] An example of such a calculation is shown in Fig. 9, for a wing of the ONERA M6 geometry. This wing has a leading-edge sweep of 30 deg, a taper ratio of 0.562, and an aspect ratio of 3.8, with 10% thick ONERA D airfoil sections. The structural model is a thin plate of the planform of the wing, discretized using 96 triangular Mindlin–Reissner finite elements, and all 168 structural DOF are kept in the time-marching aeroelastic calculations. The aerodynamic model is the fully nonlinear unsteady Euler equations. A control torque is applied (via torque tubes/actuators) at the 80% span location, oriented along the 30% chord line, and scheduled to oppose the elastic twist:

$$M_c = -K_c(\theta)\Delta\theta \tag{35}$$

where $\Delta\theta = \theta - \theta_0$ is the elastic twist of the wing from the mean steady twist θ_0, at 80% of span. The control moment M_c in Fig. 9 has been normalized with respect to the moment required to twist the wing by 1 deg, at the 80% span location. In the twist control system, K_c represents the gain associated with the wing twist feedback loop and could be considered a function of θ.

At Mach 0.84 and zero angle of attack, a plate thickness of 2.50% of root chord is required to obtain neutrally stable oscillations. The wing shown in Fig. 9 has the plate thickness of 1.8% of root chord, representing a 28% decrease in structural weight, and is, therefore, strongly unstable when the control moments are turned off ($K_c = 0$). The change in the effective damping when the twist control is activated is readily evident from the energy plot. By applying relative modest structural twisting moments, less than what is required to twist the wing tip section by 1 deg, the damping ratio of the critical aeroelastic mode has been changed from the large negative open-loop value to positive values representative of good damping.

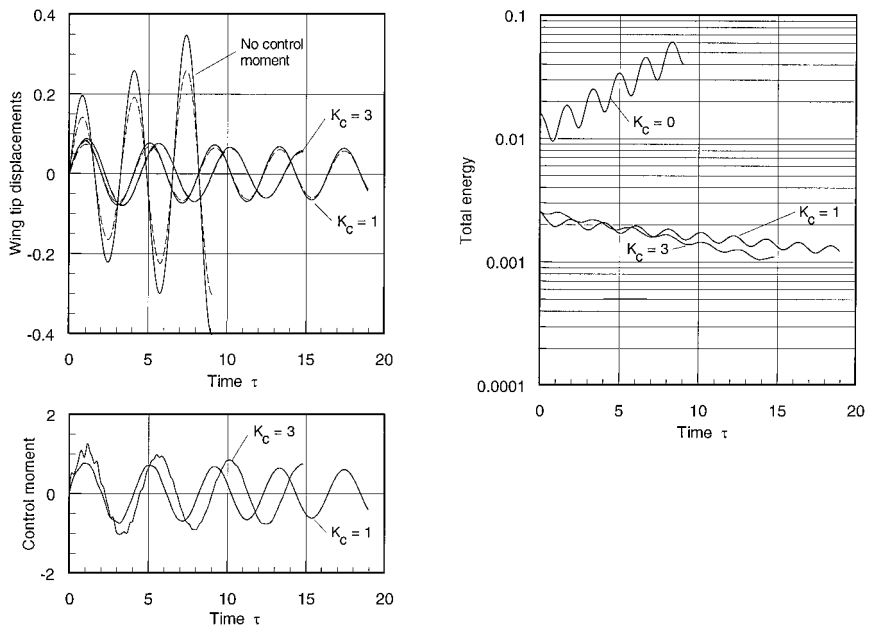

Fig. 9 Flutter suppression using aeroelastic mode control, by increasing the bending–torsion amplitude ratio using twist control; ONERA M6 wing in nonlinear transonic flow, α_∞ = 0 deg, – – –, w_{LE}, ——, w_{TE}, M_∞ = 0.84 (Ref. 13).

Conclusions

The main conclusions of this paper can be summarized as follows.

1) Bending–torsion flutter is only possible in a finite region of phase space, bounded by a closed flutter surface corresponding to neutral stability. The flutter subspace can be defined by a nonlinear aerodynamic work functional, whose magnitude represents the strength of the aeroelastic instability.

2) The aerodynamic work functional provides the basis for a new approach to the design of control laws for flutter suppression, in which the main objective is to move the system out of the unstable region of phase space, by altering the critical aeroelastic mode.

3) In the unstable region, the classical picture of frequency coalescence flutter portrayed in aeroelasticity texts may be misleading. Although the mode frequencies tend to merge as the flutter boundary is approached from below, they typically reverse direction and start to diverge once the system has crossed the flutter boundary and penetrated about 10–20% into the unstable region.

4) Calculations using the energy method predict the existence of SDOF torsional flutter for the NACA 64A006 typical section model, over a range of transonic and subtransonic Mach numbers, at moderate angles of attack (2–5 deg).

5) A new type of aeroelastic mode was discovered in the supercritical region between the flutter speed and the divergence speed. This mode is nonoscillatory and stable and corresponds to an aeroelastic eigenvalue with zero imaginary part (zero frequency) and a negative real part.

Acknowledgments

This research was supported by NASA Grant NCC 2-374 and by Air Force Office of Scientific Research Grant F49620-98-1-0302.

References

[1]Fung, Y. C., *The Theory of Aeroelasticity*, Dover, New York, 1969, pp. 170, 171.

[2]Bisplinghoff, R. L., and Ashley, H., *Principles of Aeroelasticity*, Wiley, New York, 1962, pp. 263–268.

[3]Frazer, R. A., and Duncan, W. J., "The Flutter of Aeroplane Wings," British Aeronautical Research Council R&M 1155, 1928.

[4]Garrick, I. E., "Propulsion of a Flapping and Oscillating Airfoil," NACA TR 567, 1936.

[5]Barton, M. V., "Stability of an Oscillating Airfoil in Supersonic Airflow," *Journal of the Aeronautical Sciences*, Vol. 15, No. 6, 1948, pp. 371–376.

[6]Greidanus, J. H., "Low Speed Flutter," Readers' Forum, *Journal of the Aeronautical Sciences*, Vol. 16, No. 2, 1949, pp. 127, 128.

[7]Crisp, J. D., "The Equation of Energy Balance for Fluttering Systems with Some Applications in the Supersonic Regime," *Journal of the Aero/Space Sciences*, Vol. 26, Nov. 1959, pp. 703–716, 738.

[8]Carta, F. O., "Coupled Blade-Disk-Shroud Flutter Instabilities in Turbojet Engine Rotors," *Journal of Engineering for Power*, Vol. 89, July 1967, pp. 419–427.

[9]Nissim, E., "Flutter Suppression Using Active Controls Based on the Concept of Aerodynamic Energy," NASA TN D-6199, 1971.

[10]Kousen, K. A., and Bendiksen, O. O., "Nonlinear Aspects of the Transonic Aeroelastic Stability Problem," *Proceedings of the AIAA/ASME/ASCE/AHS/ASC 29th Structures, Structural Dynamics and Materials Conference*, AIAA, Washington, DC, 1988, pp. 1–11.

[11]Bendiksen, O. O., "Nonunique Solutions in Transonic Aeroelasticity," *Proceedings of the International Forum on Aeroelasticity and Structural Dynamics*, Vol. 3, 1997, Confederation of European Aerospace Societies, Rome, pp. 425–435.

[12]Courant, R., and Hilbert, D., *Methods of Mathematical Physics*, Vol. 1, Interscience, New York, 1953, Chap. 4.

[13]Bendiksen, O. O., "Nonlinear Flutter Calculations for Transonic Wings," *Proceedings of the International Forum on Aeroelasticity and Structural Dynamics*, Vol. 2, 1997, Confederation of European Aerospace Societies, Rome, pp. 105–114.

[14]Dowell, E. H., et al., *A Modern Course in Aeroelasticity*, Kluwer Academic, Dordrecht, The Netherlands, 1995, p. 88.

[15]Lin, Y. C., Crawley, E. F., and Heeg, J., "Open- and Closed-Loop Results of a Strain-Actuated Active Aeroelastic Wing," *Journal of Aircraft*, Vol. 33, No. 5, 1996, pp. 987–994.

[16]Bendiksen, O. O., and Hwang, G., "A Flutter Control Concept for Highly Flexible Transonic Wings," AIAA Paper 97-1269, April 1997.